JOURNAL OF MAGNETIC RESONANCE **125,** 159–162 (1997)
ARTICLE NO. MN961075

Automated Shimming for Deuterated Solvents Using Field Profiling

S. SUKUMAR,*,† M. O'NEIL JOHNSON,* R. E. HURD,‡ AND P. C. M. VAN ZIJL§,¶

*Bruker Instruments, Inc., 47697 Westinghouse Dr., Fremont, California 94539; ‡G. E. Medical Systems, 47697 Westinghouse Dr., Fremont, California 94539; and §Departments of Radiology and Biophysics, Johns Hopkins University Medical School, 217 Traylor Bldg, 720 Rutland Avenue, Baltimore, Maryland 21205-2195

Received November 12, 1996

We recently demonstrated that completely automated three-dimensional image-based field mapping of high-resolution NMR samples can accomplish superior magnetic field homogeneity within a limited time period (several minutes) (*1*). Using only a few shim iterations, it is possible to shim a magnet from cryoshim to optimized shims in 15–20 min (*2*). This method is based on previously established *in vivo* principles of field mapping (*3*) and shimming (*4–8*), which were optimized for use on protonated solvents (e.g., water) in a high-resolution NMR setting. The success of this 3D approach is due to the fact that actual shim-field reference maps are generated based on the experimental shim and probe configurations, contrary to earlier approaches assuming optimized shim-field shapes based on spherical harmonics. Thus, the field over the complete sample is adjusted based on the combined effects of well-characterized local inhomogeneities and shim fields of all available shims. Contrary to hand-shim methods and FID-optimization simplex routines, this approach is insensitive to local minima, such as those frequently occuring when adjusting high-order *z* gradients based on water lineshapes. In addition, protonated samples such as water provide superb signal-to-noise, allowing rapid acquisition of 3D phase maps with excellent spatial resolution. Present 3D proton mapping uses a field of view of 28 mm in *z* and 6.4 mm in *x* and *y*, corresponding to a volume element (voxel) size of 17.5 nl for our present resolution of 64 × 32 × 32 points. In order to speed up the shimming from minutes to seconds, 1D field maps can be used for similar samples after a 3D field map has been used once to optimize all shims (*2*).

One topic that has not been addressed previously is automated shimming using deuterated solvents. Although this initially seems like a trivial extension from the principles established for protonated shimming, several additional practical problems must be solved. For instance, deuterated solvents are generally shimmed using the field–frequency lock channel, which in most high-resolution NMR machines is actually the proton coil which is also nominally tuned to the deuterium frequency. Thus, sensitivity is reduced for deuterium because the probe is optimized for protons. Furthermore, the sensitivity of an NMR experiment is proportional to $\gamma^{5/2}$, leading to an additional sensitivity loss by a factor 108 for deuterium compared to protons.

Based on these numbers, a 3D imaging approach would be too lengthy and only a 1D field profiling method can be used, limiting the useable shims to the *z* shims. This signal-to-noise issue is illustrated by the 1D field profiles along the *z* axis in Fig. 1. Because deuterated solvents are generally used by organic chemists, profiles for a tube with $CDCl_3$ are shown for a standard inverse triple-resonance probe at 500 MHz (Fig. 1A) and a standard inverse broadband probe at

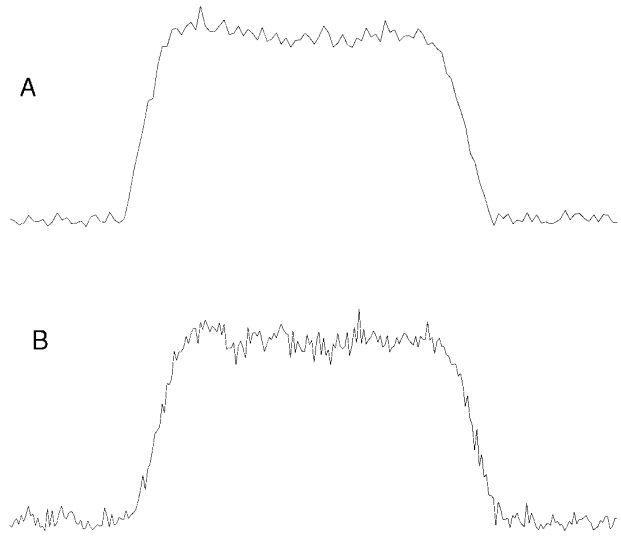

FIG. 1. One-dimensional deuterium projection along the *z* axis for a sample of $CDCl_3$ at (A) 500 MHz (4 scans, 64 points) and (B) 300 MHz (16 scans, 64 points) using a field of view of 28 mm, TR = 10 s, and TE = 5 ms. The S/N ratio is limited compared to the proton profiles obtained previously (*1*).

† Present address: Varian Associates, Inc., 3120 Hansen Way, Palo Alto, CA 94304

¶ To whom correspondence should be addressed.

1090-7807/97 $25.00
Copyright © 1997 by Academic Press
All rights of reproduction in any form reserved.

300 MHz (Fig. 1B). In order to optimize S/N with respect to maximum shimming quality and minimum experiment time, we first determined the minimum number of points needed for an accurate description of shim changes in the higher-order z shims (z^5). We found that the number of points needed for an accurate field description in these deuterium profiles is 32 or more for the region of interest. For a field of view of 28 mm and a tube diameter of 4.8 mm, this leads to a minimal voxel volume of 15.9 μl. The data for $CDCl_3$ clearly indicate that multiple scans are necessary to acquire profiles of sufficient S/N for accurate shimming.

Finally, the T_1 of these degassed organic solvents is very long, and we optimized the predelays accordingly. Using a predelay of 10 s and an approximately 70° flip angle, it was determined that 4 scans were needed for $CDCl_3$ at 500 MHz and 16 scans at 300 MHz. For other deuterated solvents (acetone-d_6, benzene-d_6, and DMSO-d_6), only a single scan was needed. Experiment timing did not improve significantly using a series of dummy scans and reduced flip angles, while shimming results degraded due to phase errors when using rapid scanning. Using a single iteration and including a 40 s time delay for data processing and storing the image file, the shimming durations for $CDCl_3$ were 2 and 6 min at 500 and 300 MHz, respectively, while it was 1 min at both fields for the other solvents.

Two more issues are important for accurate shimming of

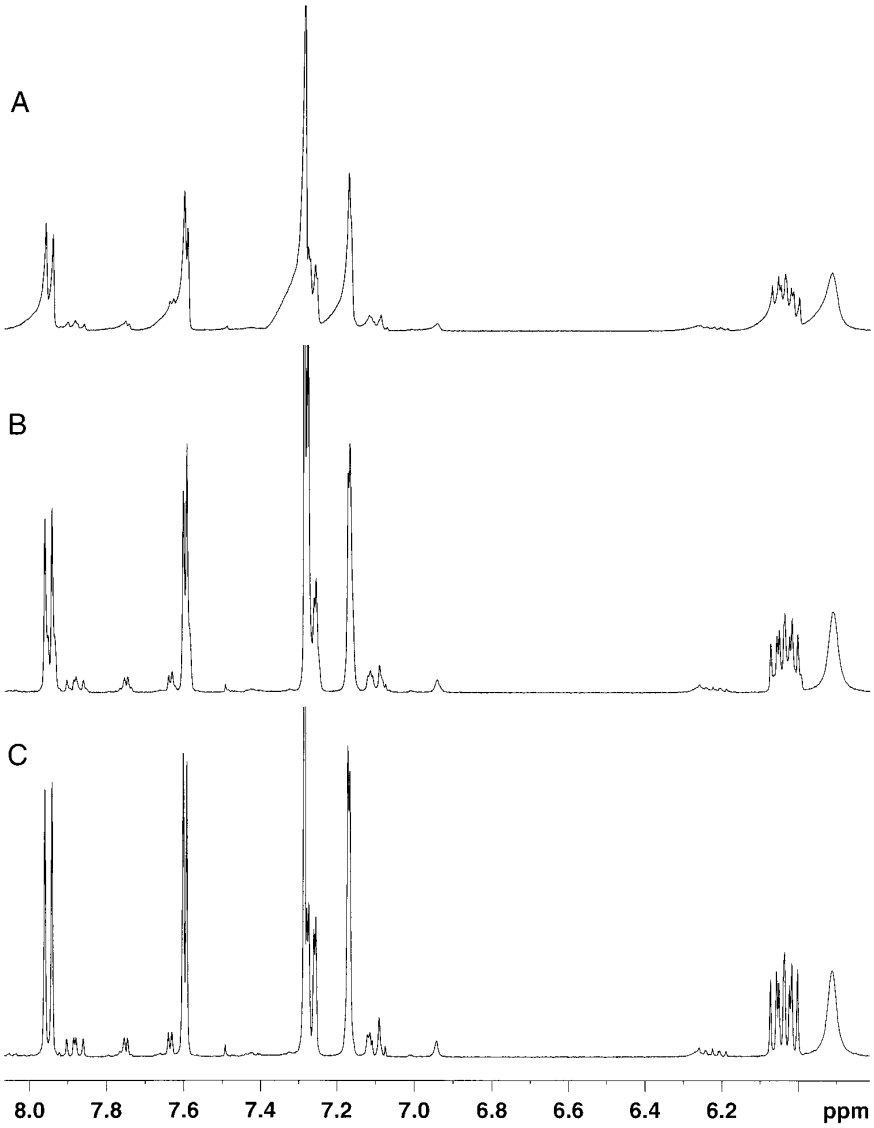

FIG. 2. Proton spectra for a sample of 16 mg/ml quinidine in $CDCl_3$ at 500 MHz (8 scans, sw 6500 Hz, 16 k real) obtained by missetting the z-z^5 shims (A), after an 8 min simplex routine for FID optimization (B), and after 2 min single-iteration gradient shimming (C).

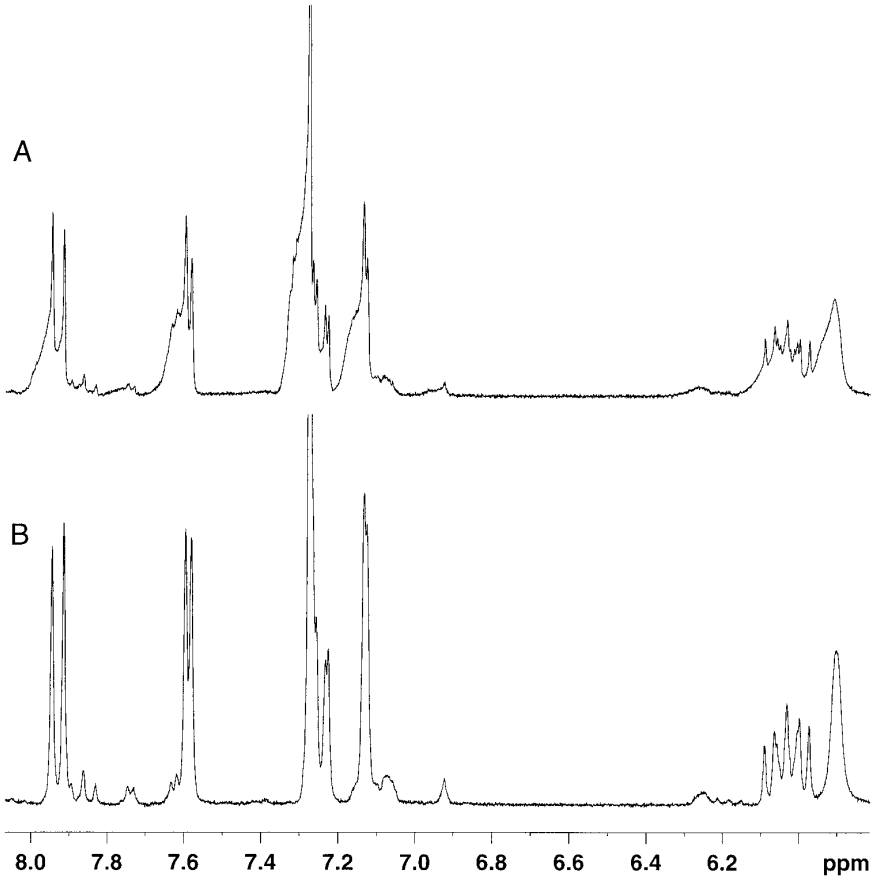

FIG. 3. Proton spectra for a sample of 16 mg/ml quinidine in $CDCl_3$ at 300 MHz (8 scans, sw 3300 Hz, 16k real) obtained by missetting the shims (A) and by single-iteration deuterium gradient shimming (B).

deuterated solvents. The first one follows directly from the equation describing the change in signal phase due to evolution of the magnetization through a field inhomogeneity $\Delta B(r)$:

$$\Delta\phi(r) = \gamma\Delta B(r)[\mathrm{TE}_1 - \mathrm{TE}_2]. \qquad [1]$$

This phase change as a function of the echo time TE depends on the gyromagnetic ratio of the nucleus. For proton shimming, we use $\mathrm{TE}_1 = 5$ ms and $\mathrm{TE}_2 = 25$ ms. In principle, the difference in TE should be a factor of 6.5 larger for deuterium, but to avoid major relaxation signal losses, we compromised to $\mathrm{TE}_2 = 75$ ms. Second, and analogously to proton shimming, care must be taken to assure that the profiles of the shim reference maps are exactly in the same location as the profiles taken to map the field inhomogeneity. This seems trivial, but it is often not realized by high-resolution spectroscopists that the profiles shift as a function of offset frequency. This shift depends on the strength of the readout gradient used in the gradient-recalled echo sequence that acquires the image (profile). To avoid these shifting problems that can completely destroy the shimming procedure, it is most straightforward to always put the solvent on resonance. For our shimming procedure, we have automated this on-resonance placement. Finally, in order to perform the deuterium shimming procedure, the console must be switched from proton acquisition to deuterium excitation and acquisition, which we also automated without need for changing any cables.

Figures 2A–2C compare the 500 MHz shim results using a simplex FID-optimization routine (Fig. 2B) and the deuterium field profiling (Fig. 2C) for a solution of quinidine (16 mg/ml) in $CDCl_3$. The obvious line broadening present when the z-z^5 shims are misset (Fig. 2A) is reduced after the 8 min simplex routine, but the lineshape is still far from perfect. After resetting the shims to the initial bad setting (Fig. 2A) and using the field profiling (2 min, single iteration), excellent lineshapes are found. Similar results were found at 300 MHz (Figs. 3A, 3B). Using different shim missetings, we found that a single 1D field profiling iteration always returned to the optimum shims reproducibly. We were not able to improve upon these shims manually. The

effect of using a different number of points to describe the field profile was also tested using spatial resolutions of 0.8, 0.4, and 0.2 mm/point. When reducing the resolution below 0.4 mm/point, the shimming procedure no longer performed optimally. Increase of the field-profile resolution to 0.8 mm/point did not significantly improve the results, and all experiments were therefore performed using 0.4 mm/point, corresponding to 64 points over our field of view of 28 mm. When reducing the number of scans for $CDCl_3$ below 4 at high field and below 16 at the low field, the shimming performance also degraded due to reduced field mapping quality at lower S/N. Also, reduction of the predelay with concommittant reduction of the flip angle did not improve the results or the experiment time (due to addition of dummy scans), and the finalized optimum field-profile data acquisition settings for $CDCl_3$ were therefore a predelay of 10 s and a number of scans of 4 and 16 at 500 and 300 MHz, respectively.

In summary, we have shown that image-based field mapping can be extended to samples in deuterated solvents. Due to the much lower S/N for deuterium, the field mapping approach is limited to a 1D approach, but we found the shim corrections (z-z^5) to be always reproducible and optimal when using off-axis shim values that were predetermined using 3D proton field mapping. Because repeat of the 3D map is not necessary, the 1D procedure allows rapid high-quality automated shimming for organic solvents, which should greatly improve present experimental results and be an important factor in high-quality reproducible automated measurement of samples not containing a strong proton signal.

ACKNOWLEDGMENT

This research is supported in part by NIH Grant RR 11115 (P.v.Z.).

REFERENCES

1. P. C. M. van Zijl, S. Sukumar, M. O'Neil Johnson, P. Webb and R. E. Hurd, *J. Magn. Reson. A* **111,** 203 (1994).
2. S. Sukumar, M. O'Neil Johnson, R. E. Hurd, and P. C. M. van Zijl, Abstracts of the Experimental NMR Conference, Boston, p. 99, 1995.
3. A. A. Maudsley, H. E. Simon, and S. K. Hilal, *J. Phys. E* **17,** 216 (1984).
4. M. G. Prammer, J. C. Haselgrove, M. Shinnar, and J. S. Leigh, *J. Magn. Reson.* **77,** 40 (1988).
5. C. Pedersen, N. Bansal, and R. L. Nunnaly, *Radiology* **173P,** 380 (1989).
6. J. Tropp, K. A. Derby, and C. Hawryszko, *J. Magn. Reson.* **85,** 244 (1989).
7. E. Schneider and G. Glover, *Magn. Reson. Med.* **18,** 335 (1991).
8. P. Webb and A. Macovski, *Magn. Reson. Med.* **20,** 113 (1991).